ACS APPLIED MATERIALS & INTERFACES

Research Article

www.acsami.org

Electrocatalytic Activity of Molybdenum Disulfide Nanosheets Enhanced by Self-Doped Polyaniline for Highly Sensitive and Synergistic Determination of Adenine and Guanine

Tao Yang,*[,†] Ruirui Yang,[†] Huaiyin Chen,[†] Fuxin Nan,[†] Tong Ge,[‡] and Kui Jiao*[,†]

[†]Key Laboratory of Sensor Analysis of Tumor Marker of Education Ministry, Shandong Provincial Key Laboratory of Biochemical Analysis, College of Chemistry and Molecular Engineering, Qingdao University of Science and Technology, 53 Zhengzhou Road, Qingdao 266042, P. R. China

[‡]Huangdao Entry-Exit Inspection and Quarantine Bureau, Qingdao 266555, P. R. China

Supporting Information

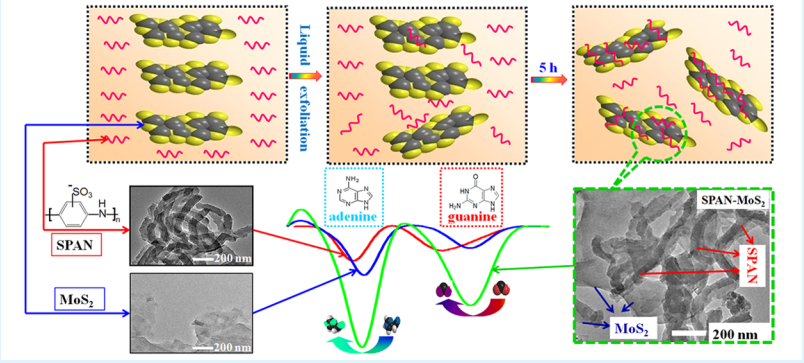

ABSTRACT: Recently, easy, green, and low-cost liquild exfoliation of bulk materials to obtain thin-layered nanostructure significantly emerged. In this work, thin-layered molybdenum disulfide (MoS_2) nanosheets were fabricated through intercalation of self-doped polyaniline (SPAN) to layer space of bulk MoS_2 by ultrasonic exfoliating method to effectively prevent reaggregation of MoS_2 nanosheets. The obtained hybrid showed specific surface area, a large number of electroactive species, and open accessible space, accompanied by rich negative charged and special conjugated structure, which was applied to adopt positively charged guanine and adenine, based on their strong $\pi-\pi^*$ interactions and electrostatic adsorption. Also, the SPAN-MoS_2 interface exhibited the synergistic effect and good electrocatalytic activity compared with the sole SPAN or MoS_2 modified electrode.

KEYWORDS: *molybdenum disulfide nanosheet, liquid exfoliation, electrochemical catalysis, self-doped polyaniline, synergistic effect*

INTRODUCTION

In the past few years, 2D thin-layered nanomaterials such as graphene and its analogues (such as molybdenum disulfide, MoS_2) have generated particular interest. These materials display unique properties and potential applications in transistors,[1,2] supercapacitors,[3] electroanalysis,[4−6] thermal conductors,[7] and so on. However, the bottleneck of these applications is the lack of an easy method to exfoliate bulk materials to thin-layered nanostructure, which attract the great passion of people.

Recently, only a few methods to acquire few-layered nanomaterials have been reported, such as mechanical exfoliation,[8,9] chemical synthesis,[10−12] and liquid exfoliation.[13−16] Among them, easy, green, and low-cost liquid exfoliation was significantly adopted to obtain thin-layered materials from their bulks. Raston et al. established a facile and versatile approach for the "top-down" fabrication of 2D sheets (such as of BN, MoS_2, and WS_2) in water stabilized by the proton rich *p*-H_2O_3P-calix[8]arene, where the calixarene is versatile, in facilitating the exfoliation as well as stabilizing the layered materials over a wide pH range.[17] They further found that pyrene-conjugated hyaluronan facilitated the exfoliation of low-dimensional nanomaterials including graphite, hexagonal boron nitride, and MoS_2 in water (and PBS solutions), with the assistance of sonication.[18] Furthermore, Notley et al. exfoliated single and few layer MoS_2 from the bulk form through a liquid phase exfoliation procedure. Highly concentrated suspensions were prepared that were stabilized against reaggregation through adsorption of nonionic polymers to the sheet surface.[19]

Under those directions, in this work, for the first time, a simultaneous intercalation and liquid exfoliation process with the help of ultrasonication and self-doped polyaniline (SPAN, a

Received: November 20, 2014
Accepted: January 14, 2015
Published: January 14, 2015

DOI: 10.1021/am5081716
ACS Appl. Mater. Interfaces 2015, 7, 2867−2872

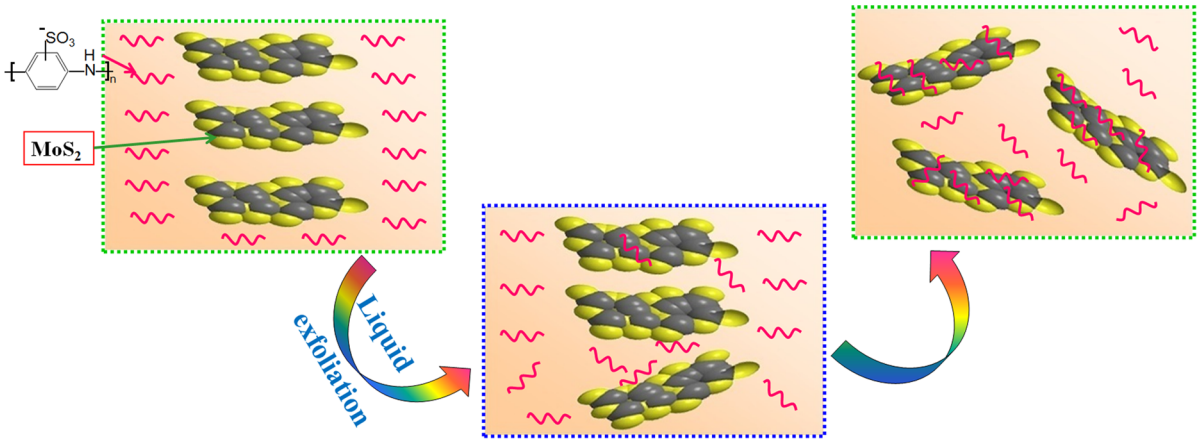

Figure 1. Simultaneous intercalation and liquid exfoliation process to form MoS_2 nanosheets.

copolymer of aniline and *m*-aminobenzenesulfonic acid) was developed to construct MoS_2 nanosheets (Figure 1) through the electrostatic repulsion between the negatively charged SPAN and MoS_2 and the strong $\pi-\pi^*$ stacking between the backbones of SPAN and the MoS_2. The fabricated MoS_2–SPAN/carbon paste electrode (MoS_2–SPAN/CPE) owns a large surface area and excellent electrocatalytic ability to detect the positive and rich-conjugated molecules, such as the free base of dexyribonucleic acid (DNA). Compared to the electrochemical performance of sole MoS_2/CPE and SPAN/CPE, extremely enhanced electrochemical responses of guanine and adenine at the surface of the MoS_2–SPAN/CPE were ascribed to the synergistic effect between MoS_2 and SPAN, which shows widest detection range from 0.05 to 100 μmol L^{-1}.

EXPERIMENTAL SECTION

Apparatus and Reagents. Electrochemical measurements were carried out by a CHI 660C (Shanghai CH Instrument Company, China). A platinum wire, a saturated calomel electrode (SCE), and CPE or modified CPE were used as auxiliary electrode, the reference electrode, and the working electrode, respectively. The KQ-500B sonifier (Kunshan ultrasonic instruments Co., Ltd.) was used for ultrasonic exfoliation, and the obtained composites were characterized via transmission electron microscopy (TEM) micrographs (JEM 2100 transmission electron microscopy) and scanning electron microscopy (SEM) (JSM-6700F machine, JEOL, Tokyo, Japan).

Bulk molybdenum disulfide (MoS_2, ≥99.0%) was obtained from BASF Chemical Co., Ltd. (Tianjin, China); *m*-aminobenzenesulfonic acid (ABSA, purity >98.0%) was purchased from Fluka; guanine and adenine were, respectively, acquired from Sigma (St. Louis, MO) and BioDee BioTech Co. Ltd. (Beijing, China).

Adenine and guanine solutions were prepared by dissolving them into 0.1 mol L^{-1} NaOH solution, and kept them in a refrigerator at 4 °C. Britton-Robinson (B-R) buffer solution was prepared according to the ref 16. Moreover, all the other chemicals were of analytical grade, and all aqueous solutions were prepared with ultrapure water from an Aquapro ultrapure water system (Ever Young Enterprises Development. Co. Ltd., Chongqing, China).

Fabrication of the Modified Electrode. The preparation of CPE was according to the method reported by Yang.[20] SPAN was synthesized on the basis of ref 21. Different mass ratios between SPAN and MoS_2 (such as 1:1, 1:2, 1:3, 1:4) were mixed, dispersed in ultrapure water, and ultrasonicated for a given time until homogeneous hybrids of SPAN-MoS_2 were formed. Then, 20 μL of the mixture was dripped on the bare CPE surface and dried in the air. The obtained electrode was noted as SPAN-MoS_2/CPE. In a similar way, MoS_2/CPE and SPAN/CPE were fabricated just without the SPAN or MoS_2 existing.

Electrochemical measurements. Cyclic voltammetry (CV) measurements were carried out in 1.0 mmol L^{-1} $[Fe(CN)_6]^{3-/4-}$ (1:1) containing 0.1 mol L^{-1} KCl with the potential scanning range from 0.6 to −0.3 V at a scan rate of 0.1 V s^{-1}.

Electrochemical impedance spectroscopy (EIS) was performed at 0.172 V from 10^5 Hz to 0.1 Hz with ac voltage amplitude of 5 mV. The supporting electrolyte was identical with that adopted in the CV measurements.

For differential pulse voltammetry (DPV), the pulse amplitude, pulse width, and pulse period were, respectively, set as 0.05 V, 0.06 s, and 0.2 s. Scan range was from 0.4 to 1.5 V.

In this assay, the reported result for every electrode was the mean value of three parallel measurements. And all the experiments were carried out at room temperature.

RESULTS AND DISCUSSION

Characterization of the SPAN-MoS_2 Hybrid. Figure 2 shows the SEM and TEM images of MoS_2, SPAN, and SPAN-MoS_2. As shown in Figure 2A, few-layer wrinkled sheets of MoS_2 are displayed. Similarly, the individual layer edge of the obtained MoS_2 is discovered from its TEM image (Figure 2B). The SPAN nanofibers interconnected and formed network nanostructures freely (shown in Figure 2C). Figure 2D shows the TEM images of irregular pure SPAN, which was stacked to form uniform fibrous structure with 90–100 nm in diameter. From Figure 2E,F, the SPAN nanofibers are adsorbed in MoS_2 nanosheets, where SPAN served as a layered space enlarger to build homogeneous and stable nanocomposite.

FT-IR Spectra of MoS_2, SPAN, and SPAN-MoS_2. The presence of functional groups on MoS_2, SPAN, and SPAN-MoS_2 can be confirmed by FT-IR measurement, which was carried out between 4000 and 400 cm^{-1}. As shown in Figure 3, the peaks at 1585 and 1499 cm^{-1} were accordant with C=C stretching deformation of quinoid and benzene rings, respectively.[22,23] The bands at 1303, 1228, and 1120 cm^{-1} that appeared at both SPAN and SPAN-MoS_2 were assigned to C—N stretching of secondary aromatic amine and the aromatic C—H in-plane bending. The characteristic peaks at 1033, 695, and 617 cm^{-1} corresponded to the O=S=O, S—O, and C—S stretching vibration, respectively.[24] The out-of-plane deformation of C—H in the 1,4-disubstituted benzene ring was also confirmed by the peaks at 799 cm^{-1}.[25] In the FT-IR spectra of MoS_2 and SPAN-MoS_2, the bands at about 540 cm^{-1} corresponded to Mo—S vibration.[26] The bond at about 3440 cm^{-1} represented stretching vibrations of O—H groups, which emerged in all MoS_2, SPAN, and SPAN-MoS_2 spectra. All the

DOI: 10.1021/am5081716
ACS Appl. Mater. Interfaces 2015, 7, 2867–2872

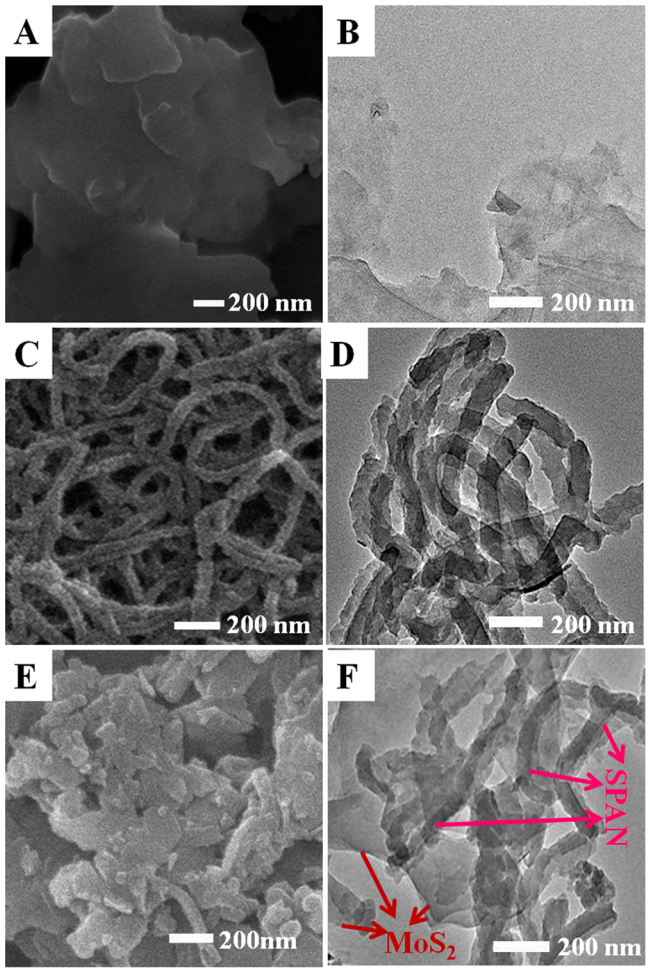

Figure 2. SEM and TEM images of MoS_2 (A, B), SPAN (C, D), and SPAN-MoS_2 (E, F).

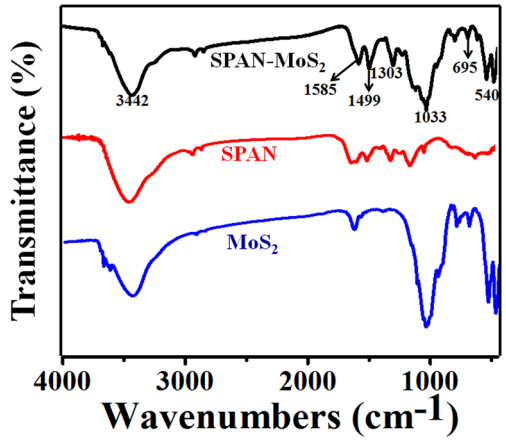

Figure 3. FT-IR spectra of MoS_2, SPAN, and SPAN-MoS_2.

results above indicated that SPAN-MoS_2 has been successfully fabricated.

Characterization of the SPAN-MoS_2 Hybrid and Synergistic Electrocatalytic Activity of Adenine and Guanine. Figure 4A exhibits CV behaviors of 1.0 mmol L^{-1} $[Fe(CN)_6]^{3-/4-}$ in 0.1 mol L^{-1} KCl at (a) CPE, (b) SPAN/CPE, (c) MoS_2/CPE, and (d) SPAN-MoS_2/CPE. In contrast to CPE (curve a) and MoS_2/CPE (curve c), SPAN/CPE (curve b) exhibits a pair of distinct redox peaks. The bare CPE and

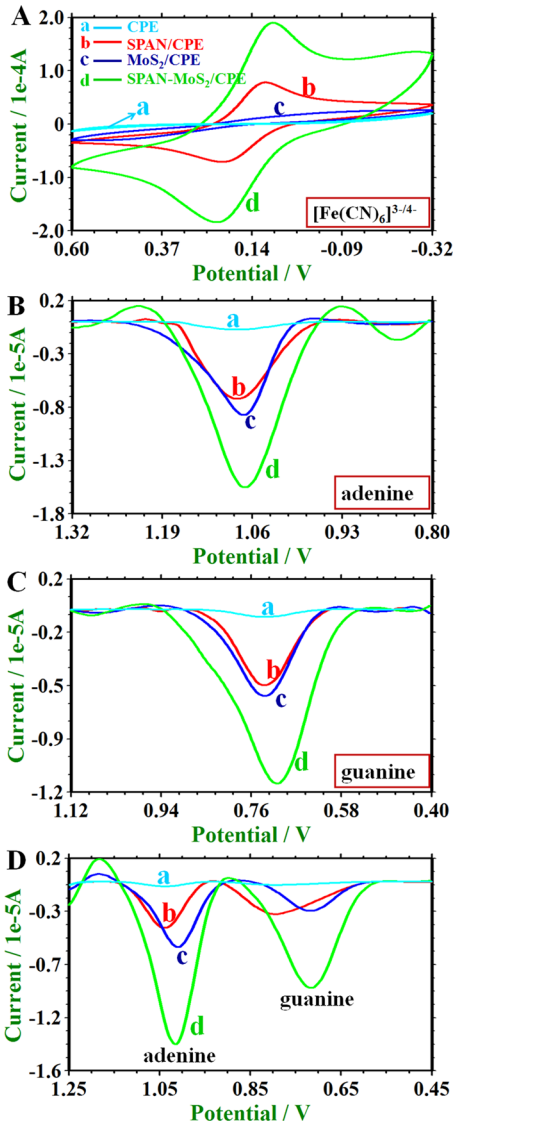

Figure 4. Representative CVs (A) of 1.0 mmol L^{-1} $[Fe(CN)_6]^{3-/4-}$ containing 0.1 mol L^{-1} NaCl. Baseline-corrected DPV of 1.0×10^{-4} mol L^{-1} adenine (B), guanine (C), and their mixture (D) recorded at different modified electrodes: (a) CPE, (b) SPAN/CPE, (c) MoS_2/CPE, (d) SPAN-MoS_2/CPE.

MoS_2/CPE do not appear in the redox peaks due to their weak conductivity. The electrochemical response of SPAN-MoS_2/CPE (curve d) reveals a more obvious oxidation peak, with the peak-to-peak potential separation (ΔE_p) of 141 mV. It demonstrated the electrochemical properties of MoS_2 could be improved by intercalating SPAN nanofibers, which was mainly attributed to the synergistic effect between MoS_2 and SPAN. Moreover, the unique nanostructure and the good electrical conductivity of SPAN-MoS_2 can facilitate the electron transfer of $[Fe(CN)_6]^{3-/4-}$, which is further confirmed by the EIS results (Supporting Information Figure S1).

Furthermore, the electrochemical behaviors of 0.1 mmol L^{-1} adenine, guanine, and their mixture in B-R buffer solution (pH 7.0) were also investigated at above-mentioned electrodes to test the catalytic activity, shown in Figure 4B–D. Compared with CPE (curve a), SPAN/CPE (curve b), and MoS_2/CPE (curve c), SPAN-MoS_2/CPE (curve d) exhibited the largest peak current. This can be assigned to the better electron

DOI: 10.1021/am5081716
ACS Appl. Mater. Interfaces 2015, 7, 2867–2872

exchange between the free bases and the electrode surface due to the strong $\pi-\pi^*$ interactions[27] and electrostatic adsorption.[28] Besides, the larger electroactive surface area also plays an important role (Supporting Information Table S1). Moreover, it enables researchers to detect adenine and guanine simultaneously for the large enough peak-to-peak separation (Figure 4D, about 296 mV). However, without guanine and adenine, there is no redox peak that appears at all the three electrodes (data not shown), implying that neither MoS_2 nor SPAN will interfere with the electrochemical response of adenine and guanine in the potential window (0.4 to 1.5 V).

Optimization of the Preparation and Determination Conditions. As shown in Figure 5, the electrochemical

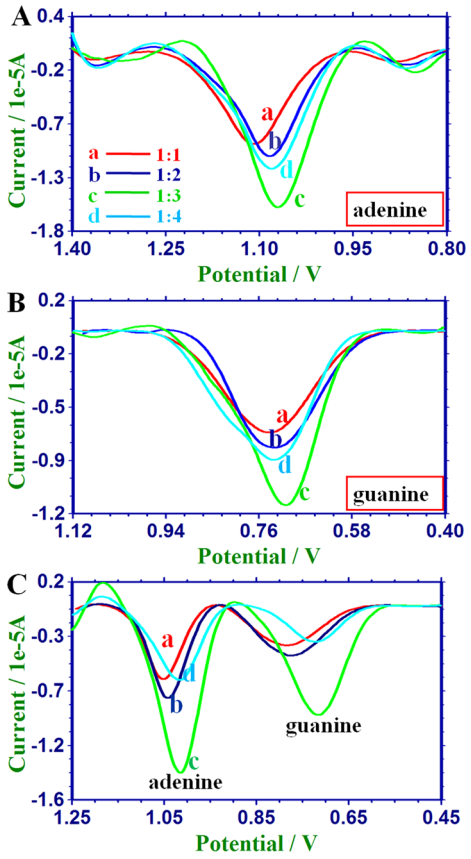

Figure 5. Baseline-corrected DPVs of 1.0×10^{-4} mol L^{-1} adenine (A), guanine (B), and their mixture (C) recorded at different mass ratio of SPAN-MoS_2 modified electrodes: (a) 1:1, (b) 1:2, (c) 1:3, (d) 1:4.

behaviors of 0.1 mmol L^{-1} adenine, guanine, and their mixture at the SPAN-MoS_2 modified electrodes obtained from different mass ratio [1:1 (a), 1:2 (b), 1:3 (c), 1:4 (d)] were investigated in B-R (pH 7.0). The oxidation peak current value (I_p) was used to evaluate the optimum mass ratio. Obviously, the SPAN-MoS_2 (1:3)/CPE (curve c) showed the largest oxidation peak currents in every solution, which was chosen as the optimal mixing mass ratio.

Next, we investigated the effect of ultrasonicaton time on the electrocatalytic behaviors of 0.1 mmol L^{-1} adenine, guanine, and their mixture. From Supporting Information Figure S2, the I_p increased accompanied by increasing the ultrasonication time of SPAN-MoS_2 composite. But after 5 h (curve c), they all decreased (curve d–e). That illustrates that the appropriate sonication will make MoS_2 nanosheets exfoliate from aggregations. Among the processes, SPAN will diffuse and intercalate in MoS_2 sheets on the basis of the strong $\pi-\pi^*$ stacking interactions between the backbones of SPAN and the MoS_2 basal planes, until all the aggregations are individually dispersed.[29] The obtained SPAN-MoS_2 composite with unique structure and rich negative charge can improve the catalytic activity of guanine and adenine, showing the largest catalytic signal (curve c). Above all, it demonstrated that the SPAN-MoS_2 composite (the mass ratio of 1:3, ultrasonicated for 5 h) modified electrode owned the largest active surface area (Supporting Information Table S1) and exhibited the best electrocatalytic activity for guanine and adenine.

With 0.1 mmol L^{-1} adenine as the typical example, the effect of pH value of B-R on the electro-oxidation of adenine at SPAN-MoS_2/CPE was also studied in the range 5.0–9.0 (shown in Supporting Information Figure S3). As we can see, the I_p increased with the pH from 5.0 to 7.0 (curve a to curve c). At pH 7.0, the maximum electro-oxidation signals appeared. With the further increase of the pH value (curve d to curve e), the peak currents decreased significantly. Hence, pH 7.0 was selected.

Determination of Individual Adenine and Guanine. Under the optimal experimental conditions, the determination of individual guanine and adenine with a series of concentrations (0.05–100 μmol L^{-1}) was investigated, respectively (shown in Supporting Information Figure S4). The typical DPVs of different concentrations of adenine were shown in Supporting Information Figure S4A; the signals increased with increasing the concentrations of adenine. Also, two linear regions were observed in the calibration curve (Supporting Information Figure S4C) with the linear regression equation as[30,31] $I_p = 2.4851C + 0.7781$ ($R^2 = 0.9893$) (0.05–1 μmol L^{-1}) and $I_p = 0.1331C + 3.7415$ ($R^2 = 0.9913$) (1–100 μmol L^{-1}). The detection limit ($S/N = 3$) was 3.0×10^{-9} mol L^{-1}.

The similar investigation was carried out about guanine, and the DPV signals were showed in Supporting Information Figure S4B. As shown in Supporting Information Figure S4D, the calibration curves revealed the similar trend from 0.05 to 100 μmol L^{-1}. The linear regression equation was as follows: $I_p = 1.9501C + 0.4734$ ($R^2 = 0.994$) (0.05–1 μmol L^{-1}) and $I_p = 0.0903C + 2.7258$ ($R^2 = 0.9932$) (1–100 μmol L^{-1}). The detection limit was 5.0×10^{-9} mol L^{-1}.

Simultaneous Detection. The electrochemical simultaneous determination of adenine and guanine was investigated under the optimized conditions (Figure 6). When the concentrations of guanine and adenine increased synchronously, two well-separated oxidation peaks, respectively, emerged at approximate +0.718 V (guanine) and +1.014 V (adenine) (Figure 6A), and the corresponding peak currents increased simultaneously. Figure 6B shows the calibration curves between the oxidation peak current value (I_p) and the concentrations of guanine and adenine from 0.05 to 100 μmol L^{-1}, which exhibited two linear segments with the regression equation as $I_p = 2.5814C + 0.6536$ ($R^2 = 0.9906$) (0.05–1 μmol L^{-1}), $I_p = 0.1105C + 3.5422$ ($R^2 = 0.9904$) (1–100 μmol L^{-1}) for adenine. The detection limit was 4.5×10^{-9} mol L^{-1}. Also, the regression equation for guanine was $I_p = 1.9130C + 0.4849$ ($R^2 = 0.9906$) (0.05–1 μmol L^{-1}), $I_p = 0.0659C + 2.7773$ ($R^2 = 0.9825$) (1–100 μmol L^{-1}) with a lower detection limit of 6.3 $\times 10^{-9}$ mol L^{-1}. Therefore, this method could sensitively and simultaneously detect guanine and adenine in a large concentration range. Our assay was also contrasted with

DOI: 10.1021/am5081716
ACS Appl. Mater. Interfaces 2015, 7, 2867–2872

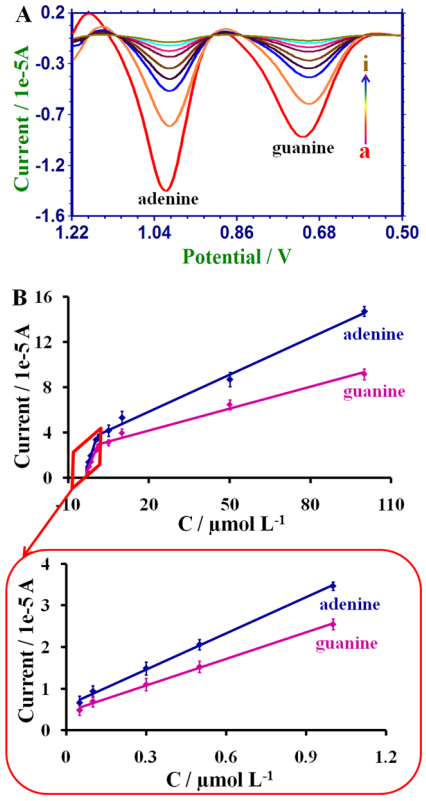

Figure 6. (A) Baseline-corrected DPVs for the simultaneous determination of adenine and guanine in B-R at SPAN-MoS_2(1:3, 5 h)/CPE with the concentration ranging from 0.05 to 100 μmol L^{-1} (from a to i: 0.05, 0.1, 0.3, 0.5, 1, 5, 10, 50, 100 μmol L^{-1}). (B) Calibration plots of the peak current versus different concentrations of adenine and guanine. Error bars are the standard deviation of three parallel experiments.

previous reports (please see Supporting Information). Supporting Information Table S2 shows our work possesses the advantages of the wider linear range and lower detection limit as compared with other earlier reports.

Stability and Reproducibility of the Modified Electrode. The stability and reproducibility of the biosensor are key factors for its further application. Also, we have demonstrated that the modified electrode has long-term stability and good reproducibility, which were shown in Supporting Information.

CONCLUSION

In summary, SPAN-MoS_2 composite was obtained through a simple technique combining intercalation and exfoliation via ultrasonication. The abundant negative charge and special structure of this hybrid made it possible to adsorb the positively charged or aromatic molecules. Due to its special properties, it is an excellent sensing platform for extensive application in catalysis detection, and biological and medical fields, such as label-free detection of single nucleotide polymorphisms of oligonucleotides.

ASSOCIATED CONTENT

Supporting Information

Details of the EIS results, electroactive surface area of the modified electrodes, the effect of ultrasonicaton time and pH value of B-R on the electrocatalytic behaviors, the determination of individual adenine and guanine, and comparison of our works and previous reports. This material is available free of charge via the Internet at http://pubs.acs.org.

AUTHOR INFORMATION

Corresponding Authors

*E-mail: taoyang@qust.edu.cn.
*E-mail: kjiao@qust.edu.cn.

Notes

The authors declare no competing financial interest.

ACKNOWLEDGMENTS

This work was supported by the National Natural Science Foundation of China (No. 21275084, 41476083), Doctoral Foundation of the Ministry of Education of China (No. 20113719130001), Scientific and Technical Development Project of Qingdao (No. 12-1-4-3-(23)-jch), and Outstanding Adult-Young Scientific Research Encouraging Foundation of Shandong Province (No. BS2012CL013).

REFERENCES

(1) Radisavljevic, B.; Radenovic, A.; Brivio, J.; Giacometti, V.; Kis, A. Single-Layer MoS_2 Transistors. *Nat. Nanotechnol.* **2011**, *6*, 147−150.
(2) Yu, W. J.; Lee, S. Y.; Chae, S. H.; Perello, D.; Han, G. H.; Yun, M.; Lee, Y. H. Small Hysteresis Nanocarbon-Based Integrated Circuits on Flexible and Transparent Plastic Substrate. *Nano Lett.* **2011**, *11*, 1344−1350.
(3) Huang, K. J.; Wang, L.; Liu, Y. J.; Liu, Y. M.; Wang, H. B.; Gan, T.; Wang, L. L. Layered MoS_2-Graphene Composites for Supercapacitor Applications with Enhanced Capacitive Performance. *Int. J. Hydrogen Energy* **2013**, *38*, 14027−14034.
(4) Sun, M. Y.; Adjaye, J.; Nelson, A. E. Theoretical Investigations of the Structures and Properties of Molybdenum-Based Sulfide Catalysts. *Appl. Catal., A* **2004**, *263*, 131−143.
(5) Huang, K. J.; Liu, Y. J.; Wang, H. B.; Wang, Y. Y.; Liu, Y. M. Sub-Femtomolar DNA Detection Based on Layered Molybdenum Disulfide/Multi-walled Carbon Nanotube Composites, Au Nanoparticle and Enzyme Multiple Signal Amplification. *Biosens. Bioelectron.* **2014**, *5*, 195−202.
(6) Huang, K. J.; Liu, Y. J.; Liu, Y. M.; Wang, L. L. Molybdenum Disulfide Nanoflower-Chitosan-Au Nanoparticles Composites Based Electrochemical Sensing Platform for Bisphenol A Determination. *J. Hazard. Mater.* **2014**, *276*, 207−215.
(7) Zhi, C. Y.; Bando, Y.; Tang, C. C.; Kuwahara, H.; Golberg, D. Large-Scale Fabrication of Boron Nitride Nanosheets and their Utilization in Polymeric Composites with Improved Thermal and Mechanical Properties. *Adv. Mater.* **2009**, *21*, 2889−2893.
(8) Xie, L.; Ling, X.; Fang, Y.; Zhang, J.; Liu, Z. Graphene as a Substrate to Suppress Fluorescence in Resonance Raman Spectroscopy. *J. Am. Chem. Soc.* **2009**, *131*, 9890−9891.
(9) Park, S.; An, J.; Jung, I.; Piner, R. D.; An, S. J.; Li, X.; Velamakanni, A.; Ruoff, R. S. Colloidal Suspensions of Highly Reduced Graphene Oxide in a Wide Variety of Organic Solvents. *Nano Lett.* **2009**, *9*, 1593−1597.
(10) Rao, C. N. R.; Nag, A. Inorganic Analogues of Graphene. *Eur. J. Inorg. Chem.* **2010**, *2010*, 4244−4250.
(11) Matte, H. S. S. R.; Gomathi, A.; Manna, A. K.; Late, D. J.; Datta, R. S.; Pati, K. C.; Rao, N. R. MoS_2 and WS_2 Analogues of Graphene. *Angew. Chem., Int. Ed.* **2010**, *49*, 4059−4062.
(12) Nag, A.; Raidongia, K.; Hembram, K. P. S. S.; Datta, R.; Waghmare, U. V.; Rao, C. N. R. Graphene Analogues of BN: Novel Synthesis and Properties. *ACS Nano* **2010**, *4*, 1539−1544.
(13) Coleman, J. N.; Lotya, M.; Neill, A. O.; Bergin, S. D.; King, P. J.; Khan, U.; Young, K.; Gaucher, A.; De, S.; Smith, R. J.; Shvets, I. V.; Arora, S. K.; Stanton, G.; Kim, H. Y.; Lee, K.; Kim, G. T.; Duesberg, G. S.; Hallam, T.; Boland, J. J.; Wang, J. J.; Donegan, J. F.; Grunlan, J. C.;

DOI: 10.1021/am5081716
ACS Appl. Mater. Interfaces 2015, 7, 2867−2872

Moriarty, G.; Shmeliov, A.; Nicholls, R. J.; Perkins, J. M.; Grieveson, E. M.; Theuwissen, K.; McComb, D. W.; Nellist, P. D.; Nicolosi, V. Two-Dimensional Nanosheets Produced by Liquid Exfoliation of Layered Materials. *Science* **2011**, *331*, 568−571.
(14) Zhou, K. G.; Mao, N. N.; Wang, H. X.; Peng, Y.; Zhang, H. L. A Mixed-Solvent Strategy for Efficient Exfoliation of Inorganic Graphene Analogues. *Angew. Chem., Int. Ed.* **2011**, *50*, 10839−10842.
(15) Huang, K. J.; Wang, L.; Li, J.; Liu, Y. M. Electrochemical Sensing Based on Layered MoS_2-Graphene Composites. *Sens. Actuators, B* **2013**, *178*, 671−677.
(16) Yang, T.; Guan, Q.; Li, Q. H.; Meng, L.; Wang, L. L.; Liu, C. X.; Jiao, K. Large-Area, Three-Dimensional Interconnected Grapheme Oxide Intercalated with Self-doped Polyaniline Nanofibers as a Free-Standing Electrocatalytic Platform for Adenine and Guanine. *J. Mater. Chem. B* **2013**, *1*, 2926−2933.
(17) Chen, X. J.; Boulos, R. A.; Eggers, P. K.; Raston, C. L. *p*-Phosphonic Acid Calix[8]arene Assisted Exfoliation and Stabilization of 2D Materials in Water. *Chem. Commun.* **2012**, *48*, 11407−11409.
(18) Zhang, F.; Chen, X. J.; Boulos, R. A.; Yasin, F. M.; Lu, H.; Raston, C.; Zhang, H. H. Pyrene-Conjugated Hyaluronan Facilitated Exfoliation and Stabilisation of Low Dimensional Nanomaterials in Water. *Chem. Commun.* **2013**, *49*, 4845−4847.
(19) Matthew, D. J.; Quinn, N. H. H.; Shannon, M. N. Aqueous Dispersions of Exfoliated Molybdenum Disulfide for Use in Visible-Light Photocatalysis. *ACS Appl. Mater. Interfaces* **2013**, *5*, 12751−12756.
(20) Du, M.; Yang, T.; Guo, X. H.; Zhong, L.; Jiao, K. Electrochemical Synthesis of Fe_2O_3 on Graphene Matrix for Indicator-Free Impedimetric Aptasensing. *Talanta* **2013**, *105*, 229−234.
(21) Zhang, C. Q.; Li, G. C.; Peng, H. R. Large-Scale Synthesis of Self-doped Polyaniline Nanofibers. *Mater. Lett.* **2009**, *63*, 592−594.
(22) He, Y. J. Synthesis of Polyaniline/Nano-CeO_2 Composite Microspheres via a Solid-Stabilized Emulsion Route. *Mater. Chem. Phys.* **2005**, *92*, 134−137.
(23) Huang, K. J.; Wang, L.; Liu, Y. J.; Wang, H. B.; Liu, Y. M.; Wang, L. L. Synthesis of Polyaniline/2-Dimensional Draphene Analog MoS_2 Composites for High-Performance Supercapacitor. *Electrochim. Acta* **2013**, *109*, 587−594.
(24) Yang, T.; Guan, Q.; Meng, L.; Yang, R. R.; Li, Q. H.; Jiao, K. A Simple Preparation Method for Large-Area, Wavy Graphene Oxide Nanowalls and Their Application to Freely Switchable Impedimetric DNA Detection. *RSC Adv.* **2013**, *3*, 22430−22435.
(25) Hu, Z. A.; Xie, Y. L.; Wang, Y. X.; Mo, L. P.; Yang, Y. Y.; Zhang, Z. Y. Polyaniline/SnO_2 Nanocomposite for Supercapacitor Applications. *Mater. Chem. Phys.* **2009**, *114*, 990−995.
(26) Liu, S. S.; Zhang, X. B.; Shao, H.; Xu, J.; Chen, F. Y.; Feng, Y. Preparation of MoS_2 Nanofibers by Electrospinning. *Mater. Lett.* **2012**, *73*, 223−225.
(27) Antony, J.; Grimme, S. Structures and Interaction Energies of Stacked Graphene-Nucleobase Complexes. *Phys. Chem. Chem. Phys.* **2008**, *10*, 2722−2729.
(28) Yin, H. S.; Zhou, Y. L.; Ma, Q.; Ai, S. Y.; Ju, P.; Zhu, L. S.; Lu, L. N. Electrochemical Oxidation Behavior of Guanine and Adenine on Graphene−Nafion Composite Film Modified Glassy Carbon Electrode and the Simultaneous Determination. *Process Biochem.* **2010**, *45*, 1707−1712.
(29) Bai, H.; Xu, Y. X.; Zhao, L.; Li, C.; Shi, G. Q. Non-Covalent Functionalization of Graphene Sheets by Sulfonated Polyaniline. *Chem. Commun.* **2009**, *13*, 1667−1669.
(30) Fan, Y.; Huang, K. J.; Niu, D. J.; Yang, C. P.; Jing, Q. S. TiO_2-Graphene Nanocomposite for Electrochemical Sensing of Adenine and Guanine. *Electrochim. Acta* **2011**, *56*, 4685−4690.
(31) Yang, T.; Kong, Q. Q.; Li, Q. H.; Wang, X. X.; Chen, L. H.; Jiao, K. One-Step Electropolymerization of Xanthurenic Acid-Graphene Film Prepared by Pulse Potentiostatic Method for Simultaneous Detection of Guanine and Adenine. *Polym. Chem.* **2014**, *5*, 2214−2218.

DOI: 10.1021/am5081716
ACS Appl. Mater. Interfaces 2015, 7, 2867−2872